J Nanostruct 10(3): 434-447, Summer 2020

RESEARCH PAPER

The Study of Photocatalytic Behavior of Carbon-ZnS Nanocomposites Prepared with Microwave Co- precipitation Method

Farnaz Maghazeii [1], Davood Ghanbari [2] , and Leila Lotfi [3]*

[1] *Mathematics and physics department, Arak Branch, Islamic Azad University, Arak, Iran*

[2] *Department of Science, Arak University of Technology, Arak, Iran*

[3] *Master of Science Student in Nano Physics, Arak Branch, Islamic Azad University, Arak, Iran*

ARTICLE INFO

Article History:
Received 14 March 2020
Accepted 29 April 2020
Published 01 July 2020

Keywords:
Carbon- ZnS nanocomposite
Co-precipitation
Mean diameter of particles
Photo-catalyst
UV-IR radiation
ZnS nanoparticles

ABSTRACT

We prepared samples including nanoparticles of ZnS via co-precipitation method in room temperature and with microwave heating using water as a "green" solvent. The procedure was repeated with various natural surfactants. XRD and SEM analysis was performed to determine the nanostructural and morphologic characteristics of nanoparticles. The mean diameter less than 100 nm for ZnS particles showed that there was well-formed pure nanostructure. SEM analysis disclosed that temperature and type of surfactant will affect the nanostructures and so we can control the nanostructure and particle size with changing such parameters. With combining of pure Carbon and ZnS nanoparticles in various proportions, Carbon - ZnS nanocomposites was prepared using microwave heating. SEM and FT-IR analysis was performed on these nanocomposites to compare them with pure Carbon and ZnS nanoparticles. We also assessed the photocatalytic potential of prepared nanocomposites using acidic and neutral pH methyl orange and Congo red solutions under UV- IR radiation. This study confirms that these nanocomposites can be used as photo-catalysts for water refinery in home and industries.

How to cite this article
Maghazeii F, Ghanbari D and Lotfi L. The Study of Photocatalytic Behavior of Carbon-ZnS Nanocomposites Prepared with Microwave Co- precipitation Method. J Nanostruct, 2020; 10(3):434-447. DOI: 10.22052/JNS.2020.03.001

INTRODUCTION

In recent years these has been increasing attention toward toxic and non-toxic pollutants that contaminating water resources [1-4]. Scientists are attempting to decontaminate water by photo-catalysts [5,6]. Semiconductor photo-catalysts are a good candidate for water refinery because they are chemically stable, with high efficiency and low cast and they are easily available [7].

Bulk ZnS is a paired semiconductor with wide energy gap (~ 3.6 eV), high refractive index and high transmittance in the visible range [1,8-10]. ZnS can produce electron-hole pairs under light radiation and act as a photo-catalyst by releasing active hydrogen radicals [11-14]. The size of ZnS particles severely affects the energy gap and surface parameters such as surface areas and surface defects [1,15,16]. Nowadays there is increasing attention toward ZnS nanoparticles because it has numerous applications in new technologies from optoelectronics to photo-catalysts.

There has been some studies to optimize synthetic conditions by changing various experimental parameters such as heating conditions and various surfactants in different concentrations to control the morphology and size of particles in ZnS nanostructures [15,17,18].

* *Corresponding Author Email: f-maghazeii@iau-arak.ac.ir*

Researchers have used several methods for preparation of ZnS nanoparticles, such as hydrothermal method [7,19], chemical vapor deposition [20], co-precipitation [21] and thermal decomposition [22]. There are several attempts to increase the efficiency and to accommodate the procedures with environmental concerns [8].

In recent years the researchers used microwave assisted co- precipitation method particles in low temperatures [9,23-25]. There are some data that show inclusion of non-metal compounds in ZnS nanoparticles can form an intermediate energy level in energy gap so it will increase the capacity of light absorption in range. Carbon is one of the best substances for enhancing the photocatalytic capacity under visible light radiation[26-29]. When the light is radiating, the electrons will be upgraded to the Carbon nanoparticles on surface of crystals, so the separation between photoelectrons and holes increases and they would not be re- combined[30-34].

In our research, at first we synthesized Zinc sulphide nanoparticles using co-precipitation method in room temperature and with microwave heating with or without the presence of a surfactant.We studied the effect of heating and the presence of surfactants on nanostructure and nanoparticle size. In second step, we used various proportions of pure Carbon for synthesize of nanocomposites in conjunction with Zinc sulphide nano particles. To determine the photocatalytic power of nanocomposites, we used the color change under UV-IR radiation of methyl orange and Congo red in acidic and neutral pH.

MATERIALS AND METHODS

Materials and devices

In this study we used $Zn(OAC)_2$, Na_2S, $C_2H_5O_2$, $C_6H_{12}O_6$, $[C_6(H_2O)_5]_6$, $NaC_{12}H_{25}SO_4$ from Merck company and distilled water from Tehran Kimia-Acid company.

Nanoparticles were synthesized by co-precipitation in room temperature and also by heating with simple kitchen microwave oven from Panasonic company with power of 600 Watt.

The synthesize of nanoparticles were repeated in room temperature and microwave in the presence of various surfactants such as SDS, gelatin, glucose and starch. To determine the structural characterization of samples, we used XRD analysis with CuKα (λ = 1.5418 Å) in the range of 2θ= 10-80°. The SEM images were obtained by LEO instrument model 1455VP. Infrared spectrophotometer was used to determine the spectrum of pure ZnS nanoparticles, pure Carbon and Carbon-ZnS nanocomposites.

nanocomposites were assessed by methyl-orange and Congo red in neutral and acidic pH under UV-IR radiation and the change of colors with respect to time were measured.

Zinc Sulfide nanoparticles synthesize

0.5 gr. of $Zn(OAC)_2$ were dissolved in 100 ml distilled water and stirred by magnetic stirren to

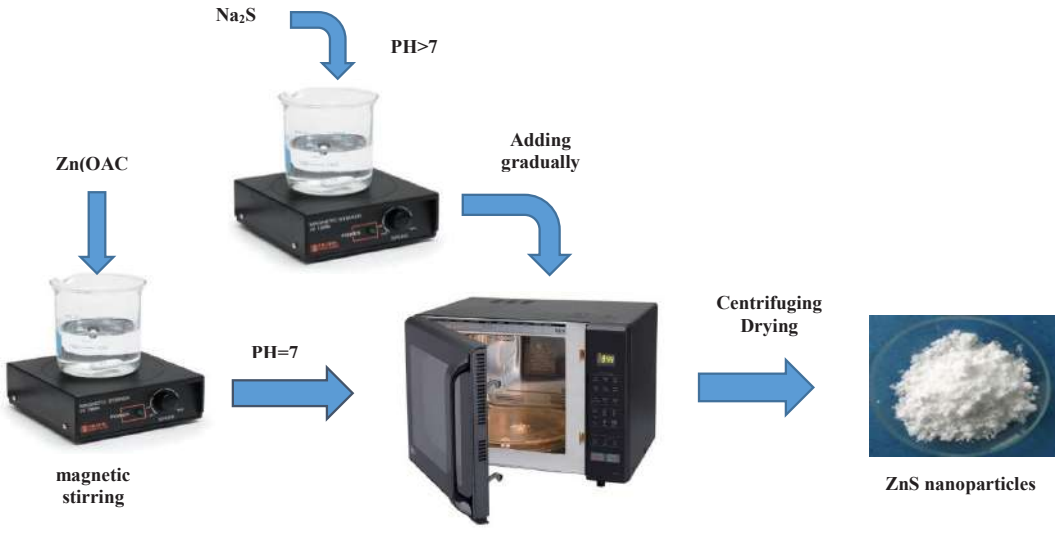

Fig. 1. Schematic of samples including ZnS nanoparticles preparation

produce a clear solution. We prepared similar solution of 0.18 gr. Na_2S in 100 ml distilled water by the same manner. The first solution had pH equal to 7 and the second was acidic. We put the Zinc acetate on a magnetic stirren and Na_2S solution was added about 10 ml every 1 min. and after that, it remained on stirren for additional 10 minutes to complete the solving process. The solution remained for several minutes on table to start the precipitation. Then we centrifuged the sample and dried it in oven. The resultant sample was used as a control sample in our study. To determine the effect of heating on nanostructure of the products, we used microwave heating during the addition of Na_2S solution, then all of products were centrifuged and dried.

Zinc sulfide nanoparticles synthesize with various surfactants

0.5 gr. of $Zn(OAC)_2$ and 0.1 gr. SDS as surfactant were dissolved in 50 ml distilled water and stirred by magnetic stirren. Previously prepared Na_2S was added in 5 phases and between them we heated the solution in microwave oven for 15 seconds. Total heating time was 75 seconds. Then the precipitation was done by centrifugation and heat drying. In another experience total volume of 50 cc Na_2S was added at once to the Zinc acetate solution and then heated for 75 sec. in microwave oven.

We repeated the same synthetic procedure with the addition of 0.7 gr. of starch, gelatin and glucose. And also the same procedures repeated with addition of surfactants in room temperature to determine the effect of heating on the nanostructure of products. Fig. 1 shows the practical algorithm how to synthesize Zinc sulphide nanoparticles with or without use of various surfactants.

Prepare of Carbon-ZnS nanocomposites

To produce pure Carbon, we burned about 1 gr. of organic substances such as starch, glucose or gelatin in 300° c heating oven. Then various amounts of Carbon were combined with constant amount of ZnS to produce various nanocomposites. To prepare ZnS solution, 0,25 gr. Zinc acetate was added to 100 ml distilled water on a magnetic stirren. Then 0.3 gr. Carbon was added and waiting about 40 min. to be completely dissolved and 0.09 gr. Na_2S in 100 ml D.W. was added gradually between heating cycles in microwave oven. Each heating cycle was about 15 seconds. Then precipitation was done by centrifugation and heat drying. We repeated the procedure by 0.15 gr. and 0.53 gr. of Carbon. Fig. 2 shows the schematic diagram for experimental setup for nanocomposite preparation used in the precipitation procedure.

RESULT AND DISCUSSION

XRD analysis results

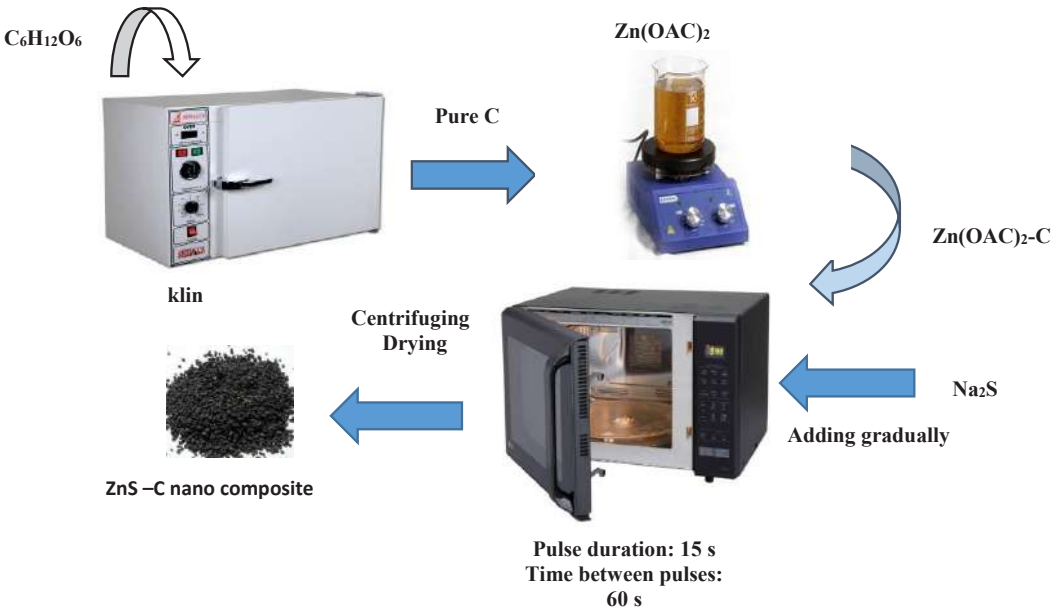

Fig. 2. Schematic of Carbon-Zinc sulphide nanocomposites preparation

Fig. 3 discloses XRD curve of control sample of ZnS nanoparticles. The XRD pattern reveals the typical diffraction pattern of pure cubic phase with F-43m space group which is consistent of pure Zinc sulphide.

Fig. 4 shows diffraction pattern of X-rays from Carbon-ZnS nanocomposites. As seen the small peaks are related to Zinc sulphide nanoparticles. The presence of narrow and pointed peaks in comparison with Fig. 3 indicates nanoparticles in nanocomposite are larger than nanoparticles in control sample.

The equation of Scherrer can determine the size of crystallines :

In this equation, β is the width of the observed diffraction peak at its half maximum intensity (FWHM), K is the shape factor, which takes a value of about 0.9, and λ is the X-ray wavelength (CuK_{α} radiation, equals to 0.154 nm). Table 1 summarizes the size of the crystallines for each peak of XRD curves. The last line shows the mean crystalline size of sample.

Generally, when the nucleation and growth comes to a balance, nanoparticles will reach to

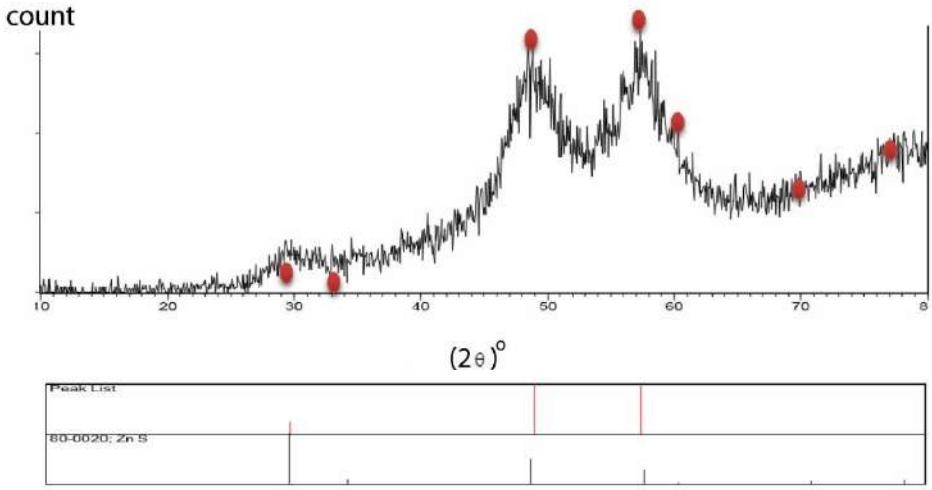

Fig. 3. XRD pattern of ZnS nanoparticles

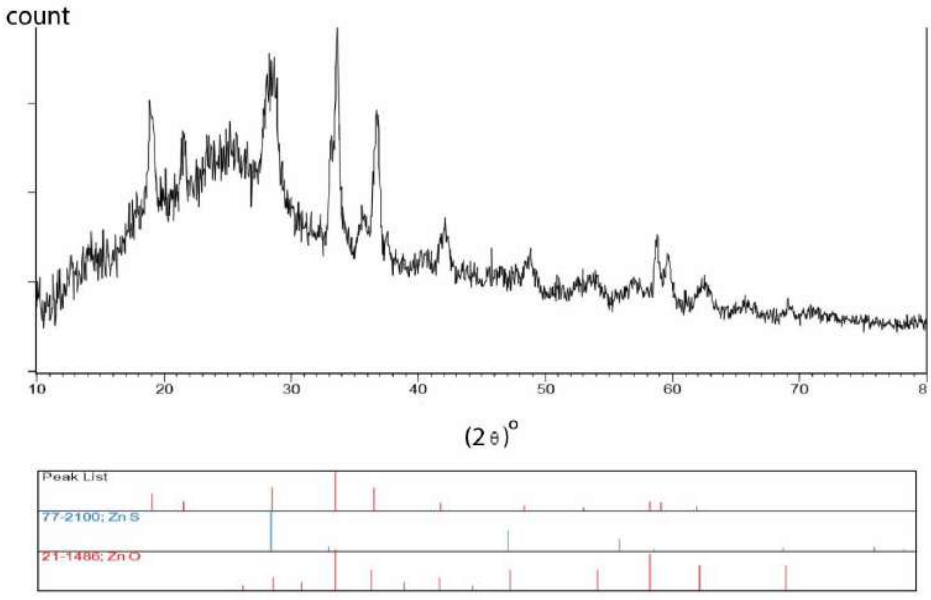

Fig. 4. XRD pattern of C-ZnS nanocomposites

their maximum size. With change in primary circumstances of synthesize, one could change the nanostructure and properties of the samples. So the properties could be controlled regarding the usage of products.

SEM analysis of samples

Fig. 5 discloses the results of SEM analysis for sample containing Zinc sulphide which prepared in room temperature and assigned as control sample. As seen, nanoparticles of Zinc sulphide have mean diameter of 48 nm. When comparing Fig. 5 with Fig. 6 which is related to SEM analysis of ZnS particles that prepared using microwave heating, one could see more uniform surface with reduced particles size (mean diameter of 36 nm) in Fig. 6.

Figs. 7 and 8 show the effect of presence of SDS as surfactant in preparation of Zinc sulphide nanoparticles in room temperature and microwave respectively which were obtained from SEM analysis. Mean diameter of nanoparticles were 44 and 42 nm respectively, which are very near to each other, but the particles prepared by microwave heating have more uniform size and smooth surface. Increased surface diffusion of particles as a result of increased temperature may be the reason for this phenomenon.

Figs. 9, 10 and 11 show the results of SEM analysis of samples prepared by microwave heating in the presence of organic surfactants of starch, gelatin and glucose respectively. Mean particle diameter were respectively 53, 49 and 53 nm. Particles formed by starch are more pleomorphic and whereas particles formed by glucose and especially gelatin are more uniform.

Table 1. The size of crystalline for each peak of XRD pattern from Scherrer equation and the mean crystalline size of sample including ZnS nanoparticles

Peak position ($2\theta^{\circ}$)	The crystalline size (nm)
29.3463	23.3
48.8482	20.5
57.3123	9.0
The mean crystalline size:	22.9

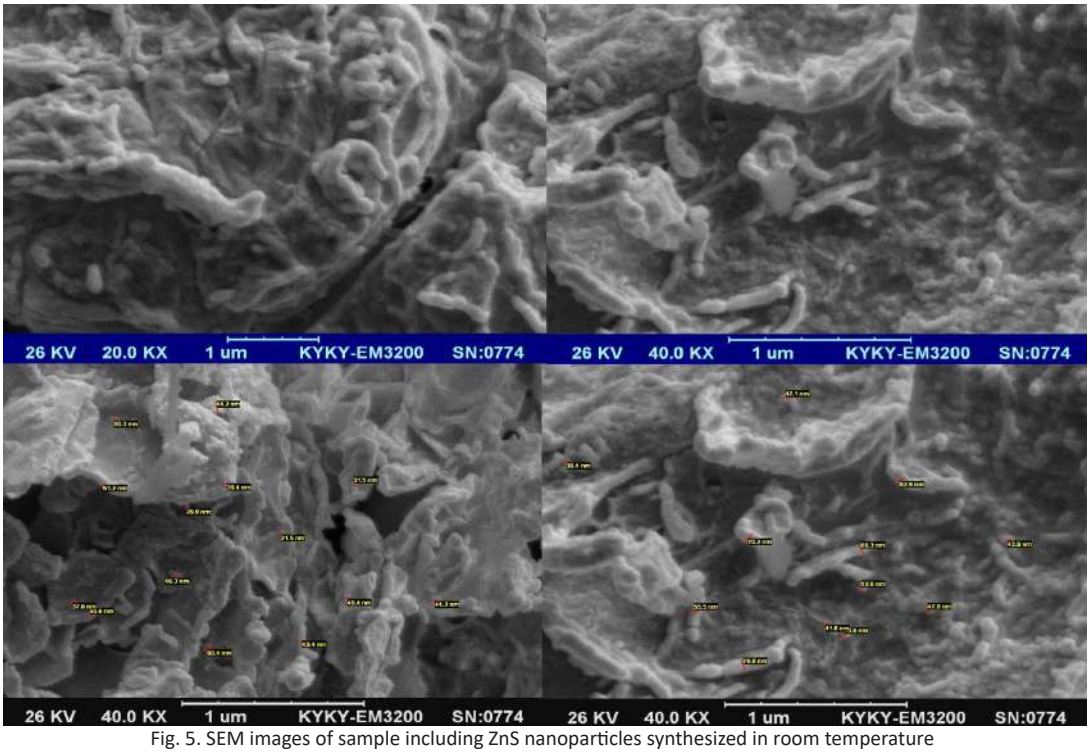

Fig. 5. SEM images of sample including ZnS nanoparticles synthesized in room temperature

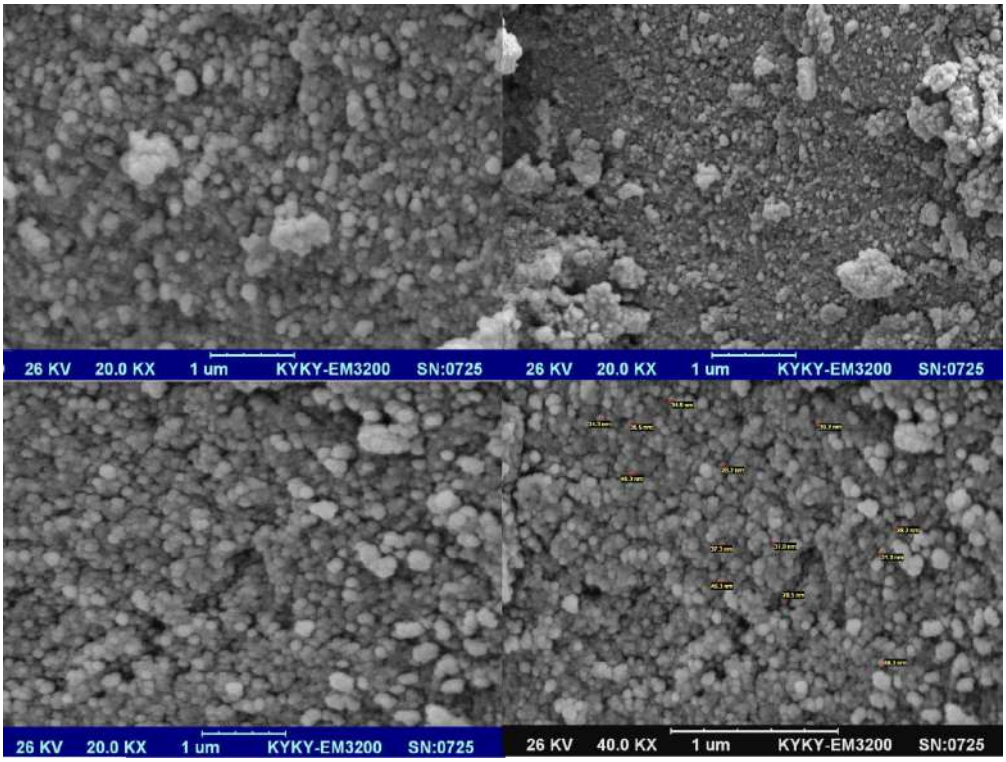

Fig. 6. SEM images of sample including ZnS nanoparticles synthesized in microwave

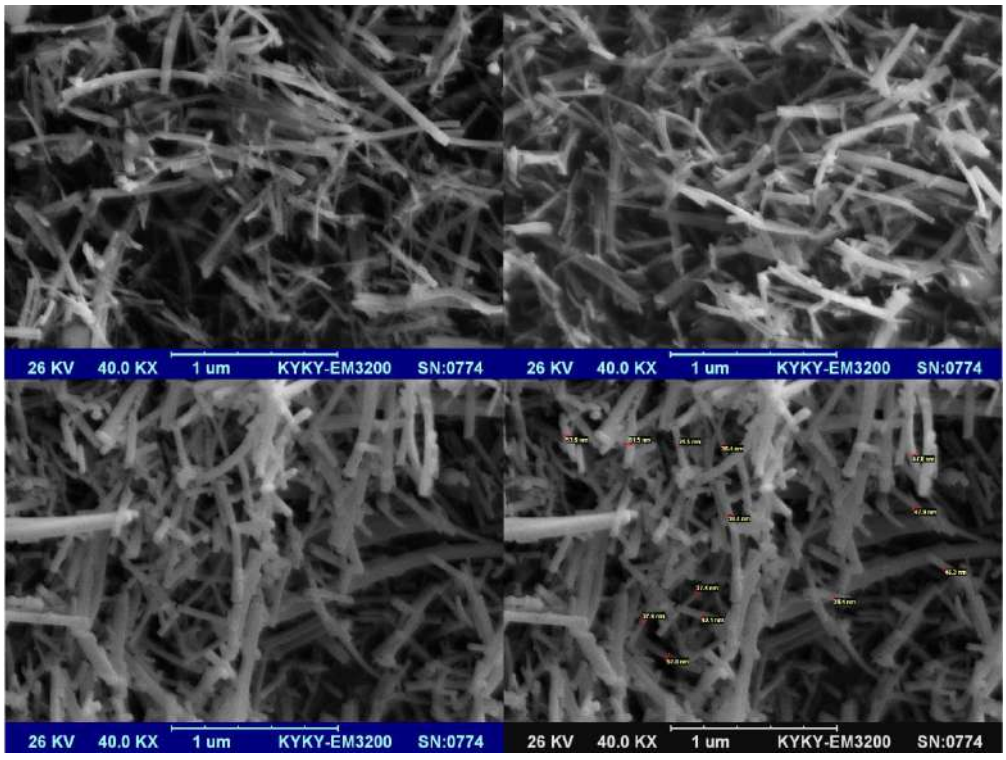

Fig. 7. SEM images of sample including ZnS nanoparticles synthesized with SDS in room temperature

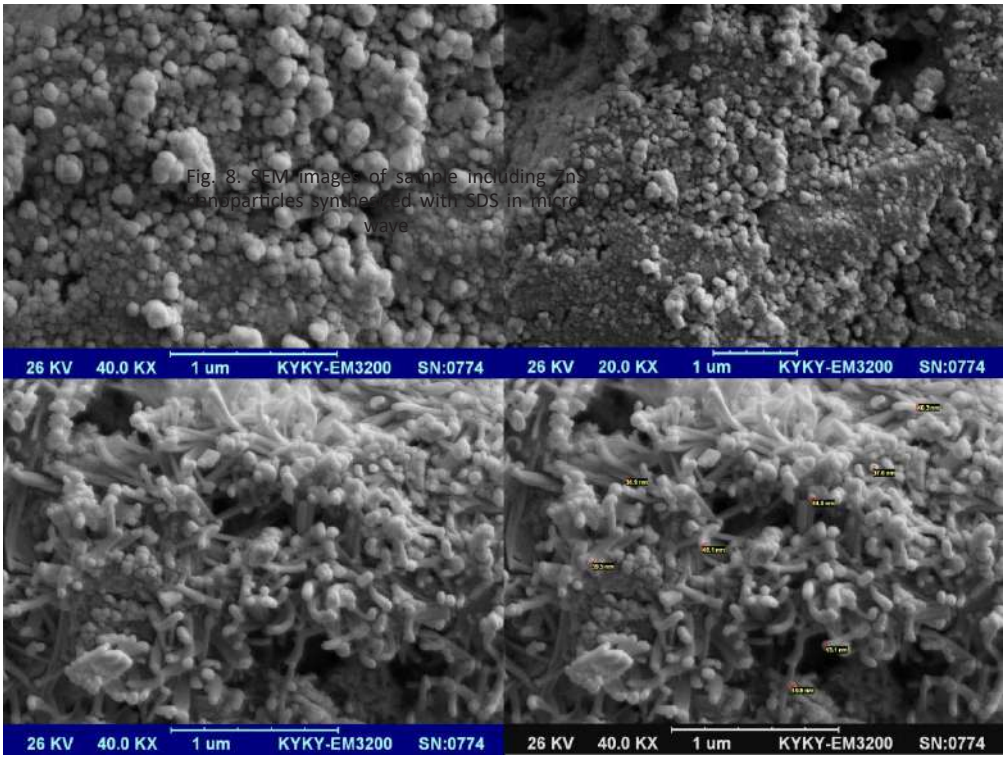

Fig. 8. SEM images of sample including ZnS nanoparticles synthesized with SDS in microwave

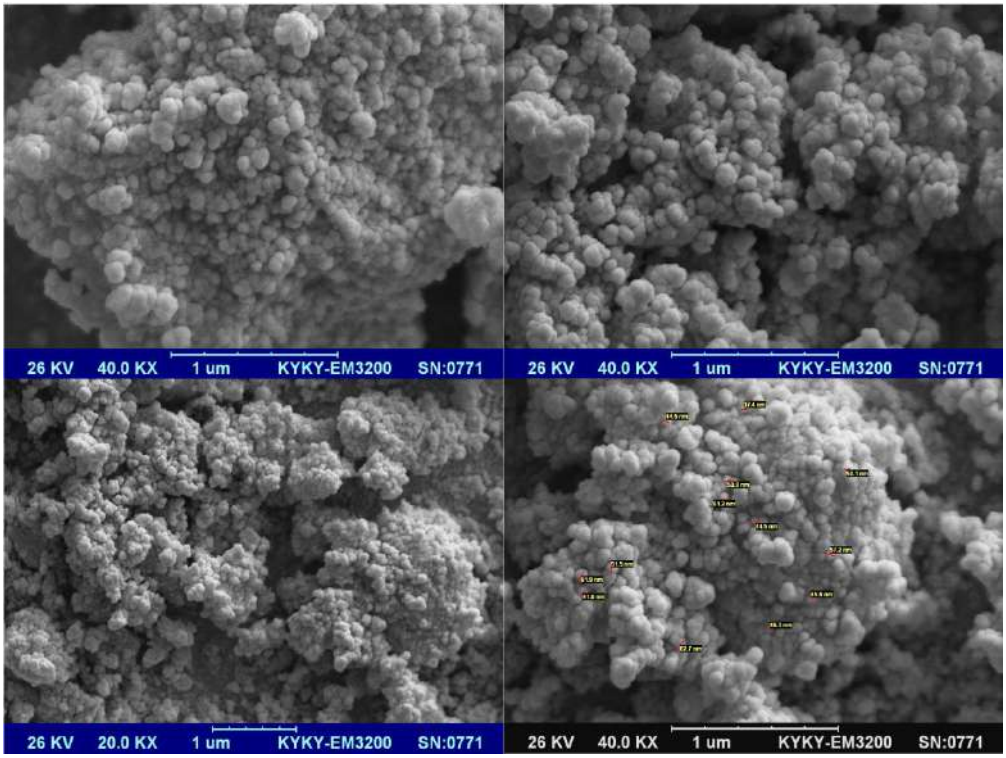

Fig. 9. The results of SEM analysis of sample including ZnS nanoparticles synthesized with starch in microwave

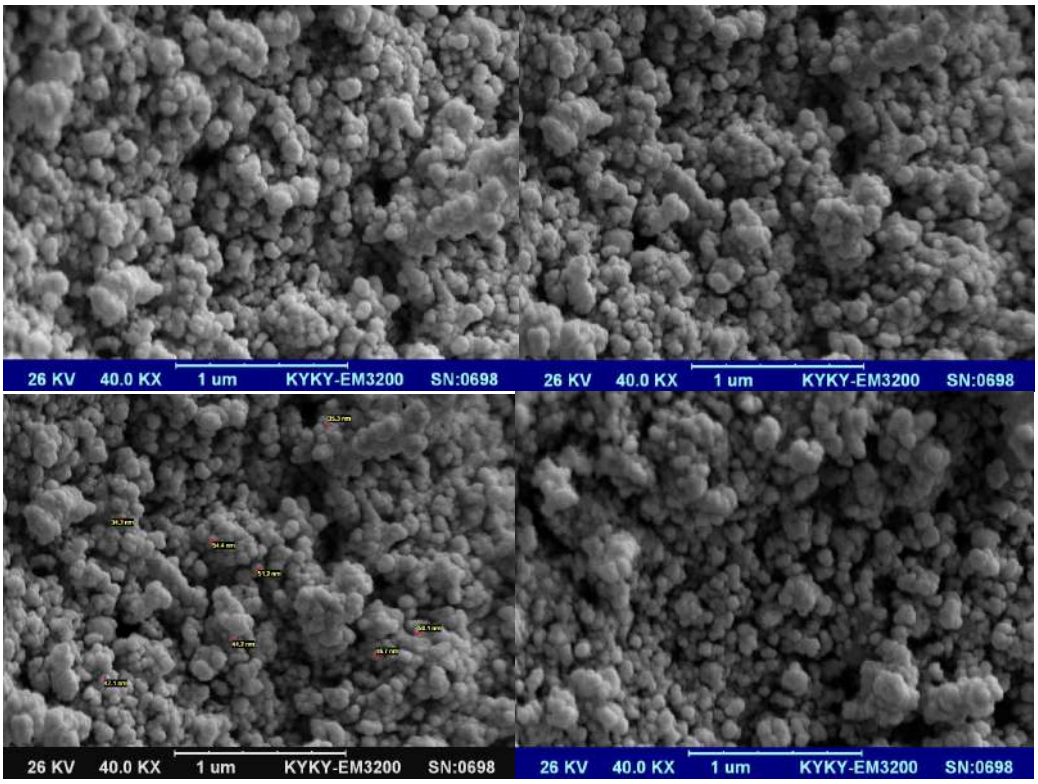

Fig. 10. The results of SEM analysis of sample including ZnS nanoparticles synthesized with gelatin in microwave

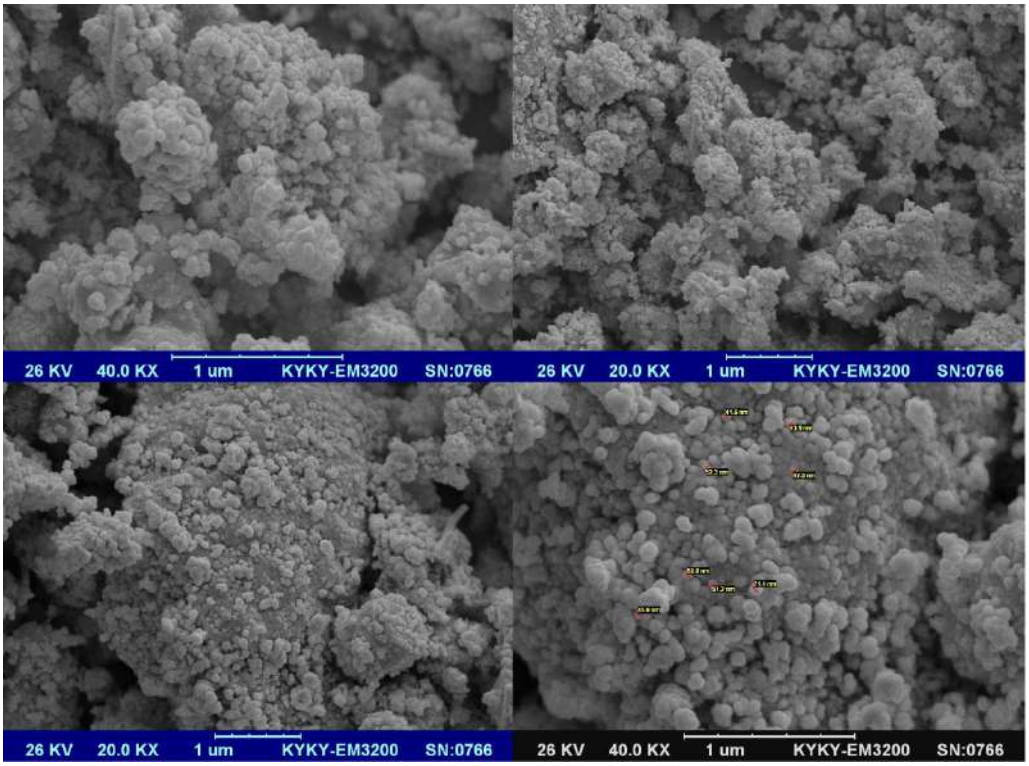

Fig. 11. The results of SEM analysis of sample including ZnS nanoparticles synthesized with glucose in microwave

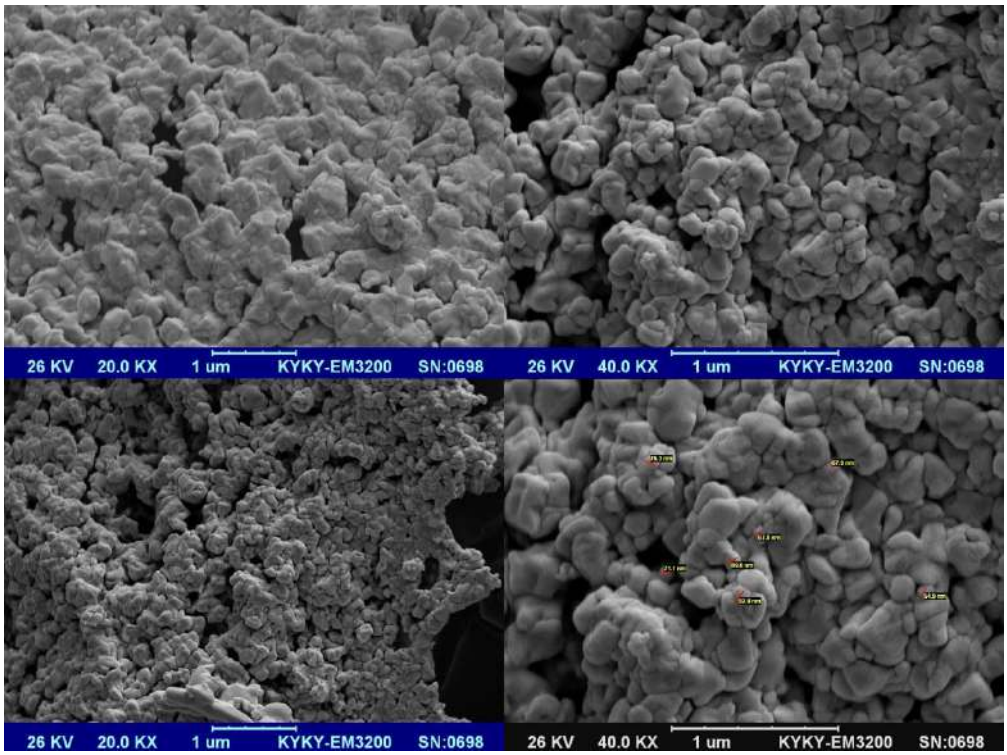

Fig. 12. SEM images of pure Carbon nanoparticles

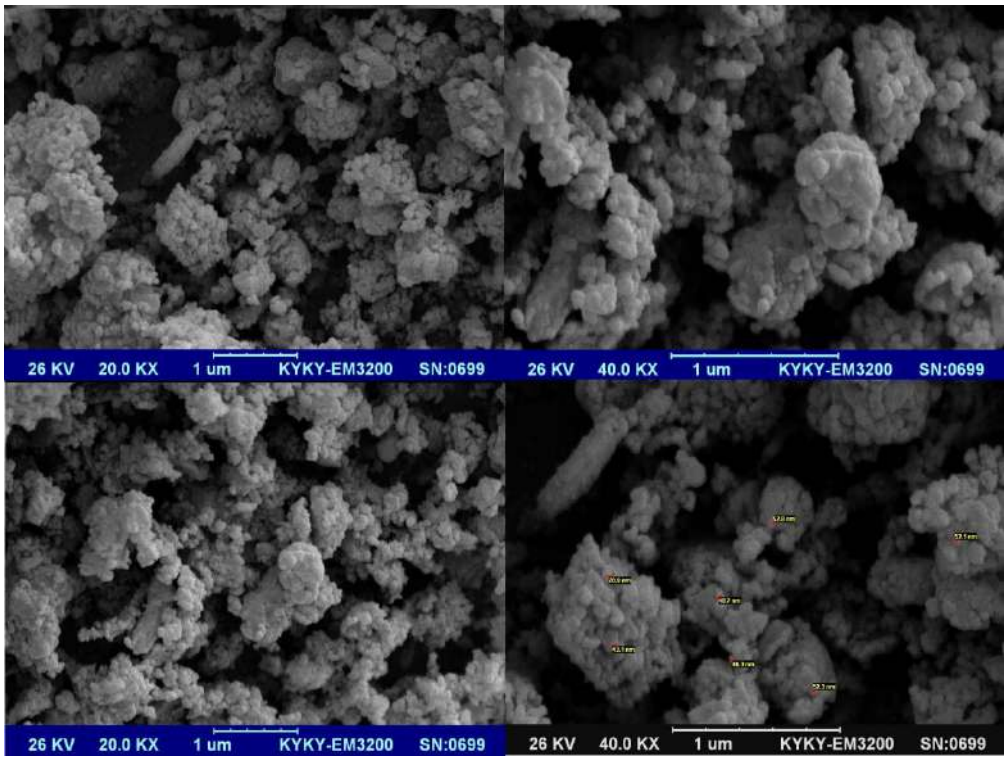

Fig. 13. SEM images of C-ZnS nanocomposites

We used pure Carbon to make Carbon-Zinc sulphide nanocomposites. Fig. 12 shows the SEM images of pure Carbon nanoparticles. It seems that there is a mixture of small and large particles in a spongy architecture with mean particle diameter of 74 nm.

Finally, Fig. 13 discloses SEM images of prepared Carbon-Zinc sulphide nanocomposite in microwave. As seen, the effect of microwave heating is the presence of reduced particles diameter with uniform surface. The mean diameter of particles is 52 nm.

Also for the samples prepared using surfactants, the best results come from SDS surfactant.

The average size less than 100 nm for particles confirms that all of our samples' nanostructure included nanoparticles.

Table 2 summarizes the results of analysis of samples containing ZnS nanoparticles and Carbon-ZnS nanocomposite.

FT-IR spectrum of samples

FT-IR spectrum of the synthesized sample ZnS nanoparticles is shown in Fig. 14. The peaks in 440,482 and 510 cm^{-1} reveal the stretching band between metal and Sulphur and the weak bands between 3300-3500 cm^{-1} are attributed O-H stretching mode due to moisture absorption on surface of nanoparticles. The band between 937-1010 cm^{-1} is assigned to C-O band that related to presence of acetate in primary substance.

FT-IR spectrum of pure Carbon nanoparticles are seen inFig. 15. The band at 3441 cm^{-1} was assigned to O –H stretching vibration mode and the

Table 2. The results of SEM analysis for all of samples

sample	RT synthesis	Microwave	synthesis	Surfactant	Mean diameter particles (nm)
ZnS	*	-		-	48
ZnS		*		-	36
ZnS	*	-		SDS	44
ZnS		*		SDS	42
ZnS		*		Starch	53
ZnS		*		Gelatin	49
ZnS		*		Glucose	53
Carbon-ZnS nanocomposite		*		-	52

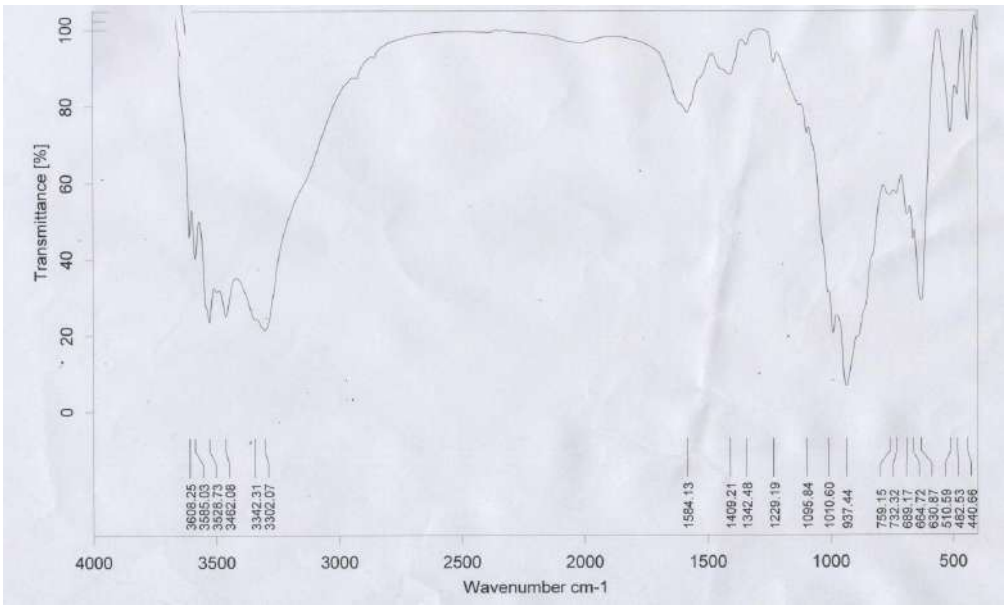

Fig. 14. FT-IR spectrum of ZnS nanoparticles

band at 1610 and 1713 cm^{-1} was assigned to the C=O stretching vibration mode. Also the narrow band at 1384 cm^{-1} is related to the resonance between C-O and C=O modes.

Finally, Fig. 16 reveals FT-IR spectrum of Carbon-Zinc sulphide nanocomposite. As it mentioned, the weak bands between 3300-3500 cm^{-1} are attributed O-H stretching mode and absorption peaks between 400-600 cm^{-1} reveal the stretching band between metal and Sulphur. The bands at 937 and 990 cm^{-1} is assigned to C-O band.

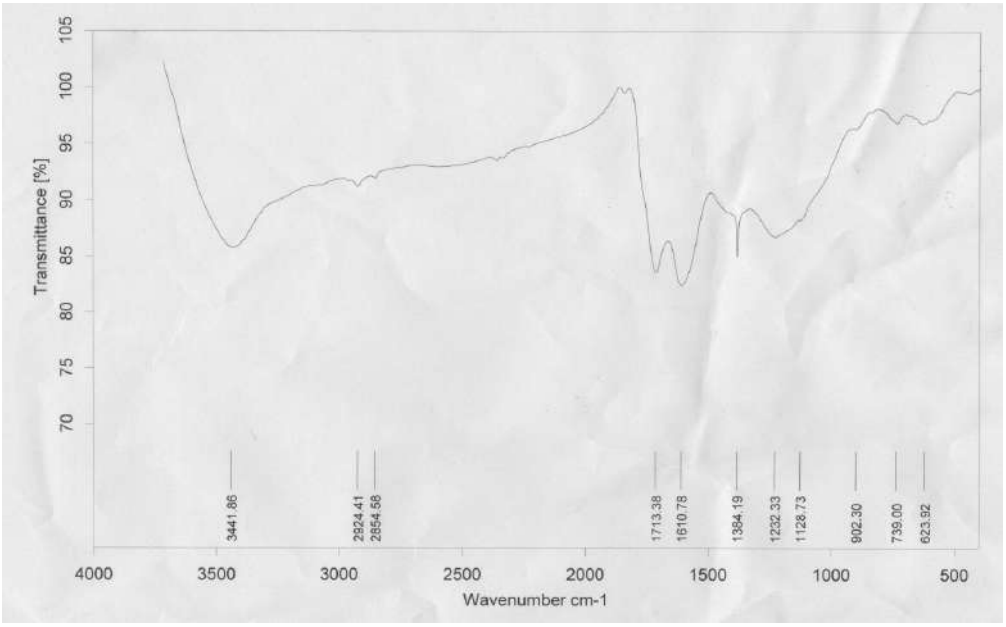

Fig. 15. FT-IR spectrum of pure Carbon nanoparticles

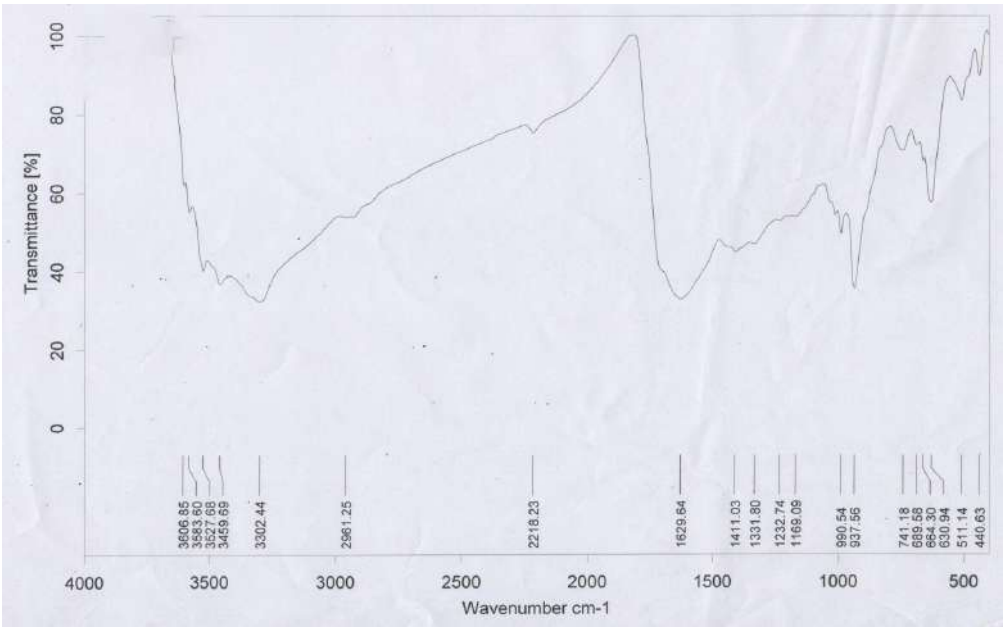

Fig. 16. FT-IR spectrum of C-ZnS nanocomposites

Photocatalytic property of Carbon-ZnS nanocomposite

Photocatalytic decontamination is one of the best methods due to absence of environmental side effects. To analyze the photocatalytic behavior of prepared nanocomposites, we used methyl orange and Congo red as natural contaminant. These dyes are widely used in photocatalytic researches due to their structural stability.

Maximum absorption peaks (λ_{max}) of these organic dyes that were used for degradation under UV light are obtained from UV-vis absorption spectra and were confirmed by scientific literature. The photo-catalytic activity of the nanocomposite's particles was evaluated by monitoring the degradation of organic dyes in acid and neutral pH in aqueous solutions, under UV-IR radiation. The changes in the concentration of dye are illustrated in Fig. 17. As time increase; more and more dyes are adsorbed on the nanoparticles catalyst, until the absorption peaks (λ_{max}) of methyl orange and Congo red decrease and almost vanish around 60 min. The dyes concentration decreased rapidly with increasing UV-IR radiation time and content of nanocomposite. Fig. 18 shows color degradation due to addition of Carbon-ZnS nanocomposite to neutral methyl orange and Congo red solutions with neutral and acidic pH under UV-IR radiation.

CONCLUSION

We synthesized various samples including Zinc sulphide plus different 5 organic surfactants with co-precipitation method in RT and under microwave heating. SEM analysis documents formation of nanostructures due to presence of mean particle diameter < 100 nm. Heating with microwave causes formation of more regular and smaller nanoparticles. Also it was evident that SDS has most powerful effect to enhance nanostructure formation and decreasing particles size of ZnS.

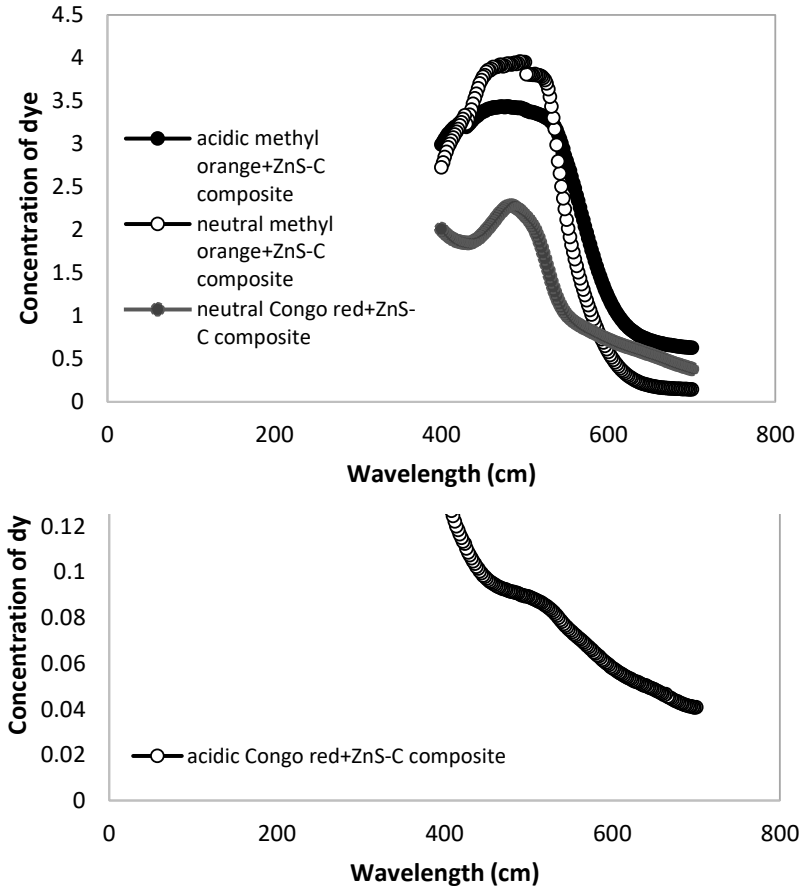

Fig. 17. The diagram of the changes in the concentration of organic dyes vs wavelength for acidic and neutral coloured aqueous solutions containing Carbon-ZnS nanocomposite under UV-IR radiation

(a) (b) (c)

Fig. 18. Color degradation due to addition of Carbon-ZnS nanocomposite to methyl orange and Congo red solutions with neutral and acidic pH under UV-IR radiation: a) neutral methyl orange b) neutral Congo red c) acidic Congo red

Also with addition of various proportions of pure Carbon to Zinc sulphide using microwave heating, it was possible to produce nanocomposites as documented by SEM analysis.

The photo-catalytic activity of the nanocomposite's particles was evaluated by monitoring the degradation of organic dyes in acidic and neutral pH in aqueous solutions, under UV-IR radiation. The dyes concentration decreased rapidly with increasing UV-IR radiation time and content of nanocomposite. This result showed that these nanocomposites are powerful tools for decontamination of household and industrial wastewater.

CONFLICT OF INTEREST

The authors declare that there is no conflict of interests regarding the publication of this manuscript.

REFERENCES

1. Lixiong Y, Dan W, Jianfeng H, Liyun C, Haibo O, Xiang Y. Morphology-controllable synthesis and enhanced photocatalytic activity of ZnS nanoparticles. J.of Alloys and Compounds, 2015; C664: 476-480.
2. Liu Y B, Li J H, Zhou B X, Lv S B, Li X J, Chen H C, Chen Q P, Cai W M. Photoelectrocatalytic degradation of refractory organic compounds enhanced by a photocatalytic fuel cell. Appl. Catal., 2012; B111-112: 485-491.
3. Satishkumar P, Mangalaraja R V, Anandan S, Ashokkumar M. CoFe2O4/TiO_2 nanocatalysts for the photocatalytic degradation of Reactive Red 120 in aqueous solutions in the presence and absence of electron acceptors. Chem. Eng. Journal, 2013; 220: 302-310.
4. Chen F J, Cao Y L, Jia D Z. A facile route for the synthesis of ZnS rods with excellent photocatalytic activity. Chem. Eng. Journal, 2013; 234: 223-231.
5. Vihmen M, Bosund M I, Kaananenc M I, Cameronc, D, Sillanpaa M. Atomic layer deposited TiO_2 films in photodegradation of aqueous salicylic acid. Sep. Purif. Technology, 2009; 66: 130-134.
6. Muruganandham M, Amutha R, Repo E, Sillanpaa M, Kusumoto Y, Abdulla-Al-Mamun M. Controlled mesoporous self-assembly of ZnS microsphere for photocatalytic degradation of Methyl Orange dye. J. Photochem. Photobiology, 2010; A216: 133-141.
7. Park J Y, Park S J, Lee J H, Hwang K J, Jin S H, Choi D Y, Yoon S D, Lee I H. Synthesis and characterization of cauliflower-like ZnS microspheres by simple self-assembly method. Mater. Lett., 2014; 121: 97-100.
8. La Porta F A, Nogueira A E, Gracia L, Pereira W S, Botelho G, Mulinari T A, Andres J, Longo E. An experimental and theoretical investigation on the optical and photocatalytic properties of ZnS nanoparticles. J.of Phys. and Chem. of Solids, 2017; 103: 179-189.
9. La Porta F A, Ferrer M M, Santana Y V B, Raubach C W, Longo V M, Sambrano J R, Longo E, Andres J, Li M S, Varela J A. Synthesis of wurtzite ZnS nanoparticles using the microwave assisted solvothermal method. J. Alloy. Compd., 2013; 556: 153-159.
10. Srinivasan N, Thirumaran S. Synthesis of ZnS nanoparticles from pyridine adducts of zinc(II) dithiocarbamates. C.R. Chimie, 2014; 17: 964-970.
11. Chang C J, Wei Y H, Huang K P. Photocatalytic hydrogen production by flower-like graphene supported ZnS composite photocatalysts. Inter. J. of Hydrogen Energy, 2017; 42(37): 23578-23586.
12. Zhang J, Yu J, Zhang Y, Li Q, Gong J R. Visible light photocatalytic H_2-production activity of CuS/ZnS porous nanosheets based on photoinduced interfacial charge transfer. Nano Lett., 2011; 11: 4774-4779.
13. Wang F, Zheng M, Zhu C, Zhang B, Chen W, Ma L. Visible light photocatalytic H_2-production activity of wide band gap ZnS nanoparticles based on the photosensitization of graphene. Nanotechnology, 2015; 26(34): 345402-(1-10).
14. Hu J S, Ren L L, Guo Y G, Liang H P, Cao A M, Wan, L J. Mass production and high photocatalytic activity of ZnS

nanoporous nanoparticles. Angew. Chem. Int. Ed., 2005; 117: 1295-1299.
15. Tian Y, Huang G F, Tang I J, Xia M J, Huang W Q, Ma Z I. Size-controllable synthesis and enhanced photocatalytic activity of porous ZnS nanospheres. Mater. Lett., 2012; 83: 104–107.
16. Soltani N, Saion E, Mat Yunus W M, Erfani M, Navasery M, Bahmanrokh G, Rezaee K. Enhancement of visible light photocatalytic activity of ZnS and CdS nanoparticles based on organic and inorganic coating. Appl. Surf. Science, 2014; 290: 440–447.
17. Lixiong Y, Dongdong Z, Dan W, Xingang K, Jiangfeng H, Feifei W, Yabo W. Size dependent photocatalytic activity of ZnS nanostructures prepared by a facile precipitation method. Materials Science and Eng., 2016; B208: 15-21.
18. Zhang S J. Preparation of controlled-shape ZnS microcrystals and photocatalytic property. Ceram. Int., 2014; 40: 4553-4557.
19. Chai L L, He W, Sun L, Jin F, Hu X Y, Ma J L. Solvothermal synthesis of wurtzite ZnS complex spheres with high hierarchy. Mater. Lett., 2014; 120: 26-29.
20. Pi Z B, Su X L, Yang C, Tian X K, Pei F, Zhang S X, Zheng J H. Chemical vapor deposition synthesis and photoluminescence properties of ZnS hollow microspheres. Mater. Res. Bull., 2008; 43: 1966-1970.
21. Srivastava R K, Pandey N, Mishra S. Effect of Cu concentration on the photoconductivity properties of ZnS nanoparticles synthesized by co-precipitation method. Mater. Sci. Semicond. Process., 2013; 16: 1659-1664.
22. Wu X C, Lai F C, Lin L M, Lv J, Zhuang B P, Yan Q, Huang Z G. Optical inhomogeneity of ZnS films deposited by thermal evaporation. Appl. Surf. Sci., 2008; 254: 6455-6460.
23. La Porta F A, Andres J, Li M S, Shambrano J R, Varela J A, Longo E. Zinc blende versus wurtzite ZnS nanoparticles: control of the phase and optical properties by tetrabutylammonium hydroxide. Phys. Chem. Chem. Phys., 2014; 16(37): 20127-20137.
24. Yan X, Michael E, Komarnenic S, Brownsond J R, Yana Z F. Microwave and conventional hydrothermal synthesis of CuS, SnS and ZnS: Optical properties. Ceram. Int., 2013; 39: 4757-4763.
25. Santana W V B, Raubach C W, Ferrer M M, La Porta F A, Sambrano J R, Longo V M, Leite E R, Longo E. Experimental and theoretical studies on the enhanced photoluminescence activity of zinc sulfide with a capping agent. J. Appl. Physics, 2011; 110: 123507-(1-8).
26. Chen L C, Tu Y J, Wang Y S, Kan R S, Huang C M. Characterization and photoreactivity of N-, S-, and C-doped ZnO under UV and visible light illumination. Journal of Photochemistry and PhotobiologyA:Chemistry, 2008; 199(2-3): 170-178.
27. Liu S, Li C, Yu J, Xiang Q. Improved visible-light photocatalytic activity of porous carbon self-doped ZnO nanosheet-assembled flowers. Cryst. Eng. Comm., 2011; 13(7): 2533-2541.
28. Zhang P, Shao C, Zhang Z. Thermal conduction and rectification in few-layer graphene Y Junctions. Nanoscale, 2011; 3(7): 2943-2949.
29. Safardoust-Hojaghan H, Shakouri-Arani M, Salavati-Niasari M. A facile and reliable route to prepare of lead sulfate nanostructures in the presence of a new sulfur source. J Mater Sci: Mater. Electron. 2015;26(3):1518-1524.
30. Ahmadian-Fard-Fini S, Salavati-Niasari M, Ghanbari D. Hydrothermal green synthesis of magnetic Fe_3O_4–carbon dots by lemon and grape fruit extracts and as a photoluminescence sensor for detecting of E. coli bacteria. Spectrochim Acta A. 2018;203:481-493.
31. Ahmadian-Fard-Fini S, Ghanbari D, Amiri O, Salavati-Niasari M. Electro-spinning of cellulose acetate nanofibers/Fe/carbon dot as photoluminescence sensor for mercury (II) and lead (II) ions, Carbohydr Polym. , 2020;229, 115428.
32. Moradi B, Nabiyouni G, Ghanbari D. Rapid photo-degradation of toxic dye pollutants: green synthesis of mono-disperse Fe_3O_4–CeO_2 nanocomposites in the presence of lemon extract. J Mater Sci: Mater Electron., 2018; 29 (13), 11065-11080.
33. Etminan M, Nabiyouni G, Ghanbari D. Preparation of tin ferrite–tin oxide by hydrothermal, precipitation and auto-combustion: photo-catalyst and magnetic nanocomposites for degradation of toxic azo-dyes. J Mater Sci: Mater Electron.. 2018;29: 1766–1776.
34. Ahmadian-Fard-Fini S, Ghanbari D, Salavati-Niasari M. Photoluminescence carbon dot as a sensor for detecting of Pseudomonas aeruginosa bacteria: Hydrothermal synthesis of magnetic hollow $NiFe_2O_4$-carbon dots nanocomposite material. Compos Part B-Eng 2019;161:564-577.